Removal of Sn²⁺ using copolymer of maleic acid-acrylic acid (PMA) by complexation-ultrafiltration and regeneration of PMA using shear induced dissociation and ultrafiltration

Huishang Le, Yunren Qiu*, Shuyun Tang

School of Chemistry and Chemical Engineering, Central South University, Changsha 410083, China, Tel. +86-15274843989, email: 1294292979@qq.com (H. Le), Tel. +86-13507479124, email: csu_tian@csu.edu.cn (Y. Qiu), Tel. +86-15074999584, email: 919503283@qq.com (S. Tang)

ABSTRACT

Commercially available polymer, the copolymer of maleic acid and acrylic acid (PMA), was used for the efficient removal of Sn^{2+} from aqueous solutions by complexation–ultrafiltration. The rejection of Sn^{2+} reached up to 99.3% at pH 5.0 and P/M (the mass ratio of polymer to metal ions) 5. The study was the first to examine the kinetics of complexation reactions of PMA with Sn^{2+}. It takes 35 min for Sn^{2+} to get the complexation equilibrium, and the reaction kinetics can be described by a pseudo-first-order equation. The stability of PMA-Sn complex in the shear field was studied for the first time. The critical rotating speeds at which the PMA-Sn complex began to dissociate were 1960, 1680, 1520 rpm at pH values 5.0, 4.0, 3.0, respectively, and the corresponding critical shear rates (γ_c) were calculated as 2.68 × 10^5, 2.15 × 10^5 and 1.67 × 10^5 s⁻¹, respectively. Furthermore, shear induced dissociation and ultrafiltration (SIDU) were effectively applied to recover Sn^{2+} and regenerate PMA. The SIDU is a promising technology for recovering tin and regenerating PMA. Compared with the traditional dissociation by acidification, SIDU avoids the use of acid and alkali, and it is in line with the idea of green chemistry.

Keywords: Copolymer of maleic acid and acrylic acid; Kinetics; Shear rate; Polymer regeneration; Shear induced dissociation

1. Introduction

Wastewater containing tin is mainly produced in electroplating, printed circuit boards, pesticides and other industries. If wastewater containing tin is discharged directly without treatment, tin ions will convert to organotin [1,2]. A large number of investigation has reported [3,4] that some organotin show specific toxic effects to different organs even at very low concentrations, which can directly damage endocrine glands, as well as altering hormone synthesis and activity of hormone receptors in the target cells. Therefore, the treatment of wastewater containing tin has aroused general attention in last few decades.

The general methodologies for the removal of heavy metal ions from wastewater are chemical precipitation, chemical coagulation, adsorption, ion exchange [5–9], etc. But these techniques are not suitable for the treatment of water steams with low concentration [10,11]. In addition, these traditional methods are difficult to achieve selective separation of heavy metals in wastewater. In past few decades, with the advantages of high efficiency and no secondary pollution, complexation–ultrafiltration process has been proved to be a promising alternative for metal removal and recovery [12–14]. It has been successfully used for treating Ni^{2+}, Zn^{2+}, Cd^{2+}, Co^{2+}, Cu^{2+}, Pb^{2+}, Hg^{2+} and other heavy metal ions in the laboratory [15–18], whereas it is relatively unexplored in recovering Sn^{2+}. In the previous studies, lots of complexing agents such as polyethylene imine [19], polyacrylate sodium [20], polyvinyl alcohol [21,22] and the copolymer of maleic acid-acrylic acid (PMA) [23], have been used in many researches. Among those, PMA owned abundant carboxyl functional groups corresponding

*Corresponding author.

to a high capacity for metal ions [23,24]. Thus, the required dosage of the copolymer is low and it is very economical. Additionally, there are several advantages of PMA, such as good water solubility, high affinity towards target metal ions, non-toxic and low cost [25]. Therefore, PMA as a complexing agent has been proved to be a promising and environment-friendly alternative.

Up to now, complexation-ultrafiltration technology has not yet applied in industry. It was reported that The Canadian Atomic Energy Research Institute has designed a pilot plant to treat toxic elements in wastewater and the rejection rate was only about 40%, far less than the laboratory effect [26]. Similarly, Tang et al. [27,28] conducted pilot experiments by different transport pumps. And it was found that the rejection of heavy metals reached nearly 100% (using the peristaltic pump) but the removal efficiency was only 45% (using a centrifugal pump) in the same membrane module. The reason was that the dissociation of the polymer-metal complex at the high shear rate generated by the blades of the centrifugal pump, resulting in a remarkable reduction of the metal rejection [29]. In order to prevent excessive shear rate, the choice of suitable centrifugal pump is a key problem that must be solved in the industrial application of complexation-ultrafiltration.

For guiding the choice of centrifugal pump parameters in the complexation-ultrafiltration process, our study tries to simulate the centrifugal pump with high shear by rotating disk membrane (RDM) module and discuss the relation between the shear rate and stability of polymer-metal complex. Furthermore, based on the fact that polymer-metal complex will dissociate exceeding a certain speed, a new technology which is shear induced dissociation and ultrafiltration were applied to recover Sn^{2+} and regenerate PMA. The traditional method of the polymer regeneration is acidification dissociation [30–32]. Compared with acidification dissociation, shear induced dissociation avoids the consumption of acid and alkali, and it is in line with the idea of green chemistry.

In this work, the kinetics of complexation reaction between PMA and the metal ions was firstly investigated to understand the time of complexation equilibrium. And then, the effect of PMA on removing Sn^{2+} was studied to obtain optimal conditions of removal. Further work was to explore the stability of PMA-Sn complex in the shear field. The research has calculated valuable data about critical shear radius and the corresponding critical shear rates; so as to lay the foundation for the following shear induced dissociation and ultrafiltration. Finally, shear induced dissociation and ultrafiltration were applied to recover Sn^{2+} and regenerate PMA. This works aim to provide the theoretical guidance for the industrialization of the removal and recovery of metal ions by complexation-ultrafiltration.

2. Experimental

2.1. Apparatus, chemicals and membranes

The experimental set-up is shown in Fig. 1a. The feed solution is circulated from a 4 L thermostatic tank to the filtration chamber by a peristaltic pump at a flow-rate 30 L/h. Feed inlet was located at 70 mm from the center on the upper plate while the retentate outlet was at the center on the bottom plate. Permeate was forced through the membrane under pressure and collected in a beaker placed on an electronic scale, while the retentate was returned to the feed tank. The rotating disk membrane module is made up with a metal rotating disk with six rectangular vanes inside a cylindrical housing. A flat membrane, with an effective area of 0.0253 m^2 (outer radius is 0.088 m, inner radius is 0.005 m), was fixed on the cover of the cylindrical housing in front of the disk. The rotating disk can rotate at adjustable speeds ranging from 0 to 3000 rpm and induce the shear rate on the membrane. Fig. 1b shows the schematic of a disk with six rectangular vanes. All experiments were performed at 25°C.

Copolymer of maleic acid and acrylic acid (PMA, M_W = 70 kDa) was supplied by Shenyang Xingqi Daily Chemicals Plant, China. $SnSO_4$ provided by Shanghai Chemical Reagent Station (China) was used as source of Sn^{2+}. The concentrations of Sn^{2+} is 10 mg/L unless special illustration. The solution pH was adjusted by adding hydrochloric acid (0.1 mol·L^{-1}) or sodium hydroxide (0.1 mol·L^{-1}). All chemi-
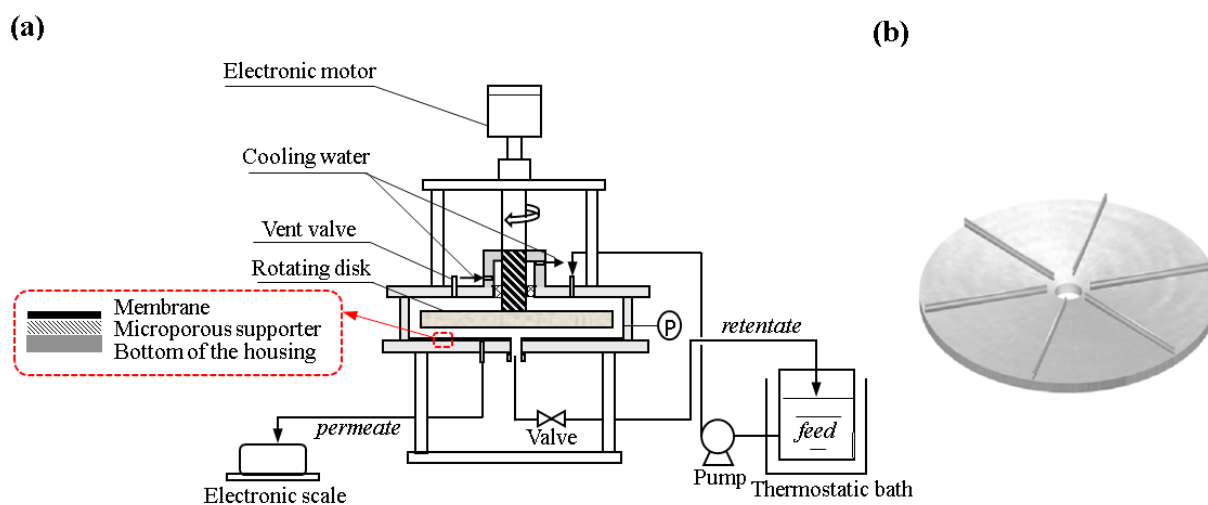

Fig. 1. Schematic of (a) experimental set-up (b) rotating disk with six rectangular vanes.

cals were of analytical grade. The ultrapure water was used throughout the experimental runs. PES flat ultrafiltration membrane with molecular weight cut-off (MWCO) 10 kDa was provided by Shanghai Yuling Filter Equipment Co, Ltd.

2.2. Pretreatment of the PMA

The structure of PMA is shown in Fig. 2, it is a copolymer made of maleic acid and acrylic acid. The only existing functional group is carboxyl group. Although the average molecular weight of the PMA is 70 kDa, there is still a small amount of PMA whose molecular weight is smaller than MWCO (10 kDa). If the copolymer solution is not pretreated in ultrafiltration process to eliminate low fractions, the copolymer with low molecular weight will permeate the membrane along with the bound metal ions, causing the decrease of metal rejection rate. Therefore, PMA solution was pretreated by the PES flat ultrafiltration membrane until no copolymer was detected in the permeate. All the following experiments were carried out with the using of pre-treated copolymer solution.

2.3. Experimental procedures

2.3.1. Kinetics experiments

The feed solution of Sn^{2+} prepared as 10 mg L^{-1} in advance was introduced to the 4 L feed tank and circulated through the apparatus. In the total recirculation process, both permeate and retentate stream were returned to the feed tank so that the concentration of feed was constant. The feed solutions were run for 1 h in the ultrafiltration system to eliminate adsorption of Sn^{2+} by membrane. Sn^{2+} concentrations in the permeate was measured to obtain the initial concentrations. Then, a large excess of PMA was added to the feed tank. The pH of the mixture was adjusted to 5.0. Once the complexation reactions started, the Sn^{2+} concentrations vs. time were obtained by means of measuring concentrations in the permeate at different time periods.

2.3.2. Total recirculation experiments

The ultrafiltration tests are carried out in full recycle process. Prior to the ultrafiltration experiments, the desired amounts of $SnSO_4$ and pre-treated PMA were dissolved separately in ultrapure water at a certain P/M, and then they were mixed to form 4 L feed solution. This feed mixture was fully stirred for 40 min (according to kinetics experiments) to insure that the complexation equilibrium between the Sn^{2+} and PMA was reached. The pH of the mixture was adjusted to a desired value during the mixing period. For
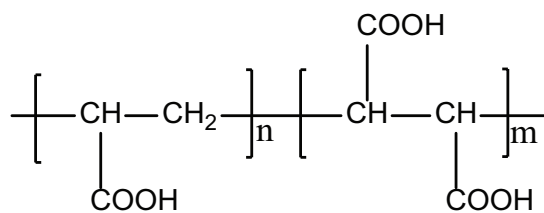

Fig. 2. Structure of the PMA.

each series of experiments, with the same membrane and test fluid, and permeate and retentate stream were returned back to the reservoir to keep the concentration constant in the feed. The system was run under the desired rotating speed and trans-membrane pressure. 3 ml sample of permeate and retentate streams was collected to determine metal concentration. The concentrations of Sn^{2+} and PMA are severally analyzed by atomic absorption spectrophotometry and total organic carbon (TOC). All tests were repeated at least three times. The errors were controlled below 5%.

2.3.3. SIDU experiments

The 10 mg L^{-1} Sn^{2+} fully reacted with PMA about 40 min under the optimum conditions, the resulting solution was placed into a 4 L feed tank and the ultrafiltration was started. And then the recovery of PMA and Sn^{2+} can be achieved by controlling proper rotating speed of rotating disk. In the experiments, permeate was discharged and collected, and the deionized water was make up to the feed tank so that the volume of the raw liquid was constant. The recovery efficiency was determined by measuring the concentration of Sn^{2+} in the retentate.

3. Results and discussions

3.1. The kinetics of complexation reaction of PMA with Sn^{2+}

The kinetics of complexation reaction for PMA and Sn^{2+} was investigated under a large excess of PMA and a constant pH 5.0. The kinetic curve of the complex formation of PMA with Sn^{2+} is presented in Fig. 3. It was found that free Sn^{2+} in the retentate decreases with the increase of the reaction time, reaches a minimum value and maintains unchanged. Eventually, it takes about 35 min for Sn^{2+} get to the complexation equilibrium. This is similar to the [13], studied the kinetics of complexation reactions for PAAS with Hg^{2+} and Cd^{2+}.

Since the rate of complex formation depends on the concentration of metal ions, ligands and hydrogen ions, the formation rate of the PMA-Sn complex can be assumed Eq. (1) based on the theories of chemical reaction rates [33].

$$-\frac{dC_{Sn}}{dt} = k(C_{Sn})^a (C_{PMA})^b \left(C_{H^+}\right)^c \tag{1}$$

where t is the reaction time, k is the rate constant, a, b and c are the reaction orders.

Under a large excess of the PMA and at a constant pH value, the reaction rate can be expressed as:

$$-\frac{dC_{Sn}}{dt} = k^*(C_{Sn})^a \tag{2}$$

where k^* is the observed rate constant, assuming $a = 1$, the rate equation for the formation PMA-Sn complex can be written as follows:

$$-\frac{dC_{Sn}}{dt} = k_1 C_{Sn} \tag{3}$$

where k_1 is the pseudo-first-order rate constant. By integrating Eq. (3), taking $t = 0$ to t and $C_{Sn} = (C_{Sn})_0$ to $(C_{Sn})_t$ into con-
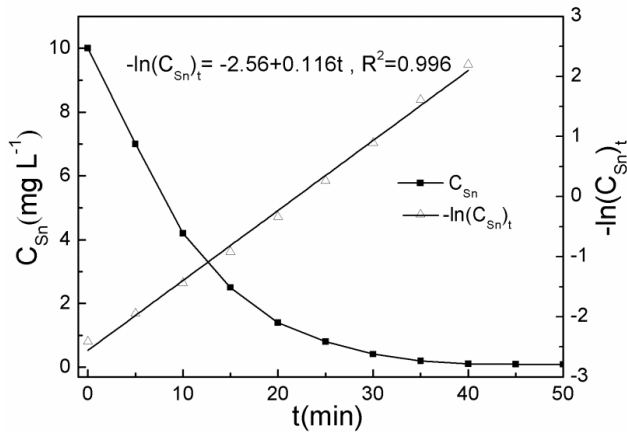
Fig. 3. Kinetic curve for the formation of PMA-Sn complex and relation of $-\ln(C_{Sn})_t$ vs. time (pH, 5.0; initial Sn^{2+} concentration, 10 mg L^{-1}; initial PMA concentration, 2000 mg L^{-1}; temperature, 25°C; initial pressure, 10 kPa).
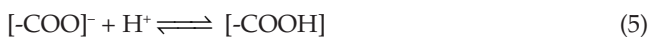

Fig. 4. Effect of pH on the rejection of Sn^{2+} at different P/M (initial Sn^{2+} concentrations, 10 mg L^{-1}; rotating speed, 300 rpm; temperature, 25°C; initial pressure, 10 kPa).

sideration, Eq. (4) can be derived. Where $(C_{Sn})_0$ is the initial concentration of tin.

$$-\ln(C_{Sn})_t = -\ln(C_{Sn})_0 + k_1 t \tag{4}$$

The plot of the relation of $-\ln(C_{Sn})_t$ vs. time was prepared via the datum was fitted according to a line, which is shown in Fig. 3. It can be seen that the value of $-\ln(C_{Sn})_0$ is –2.56 and the regression coefficient (R^2) of the fit is 0.996, suggesting that the rates of complexation reaction for PMA with Sn^{2+} was first order, and the pseudo-first-order rate constant was obtained to 0.116 min^{-1}.

3.2. Preliminary test: selection of pH and P/M

The effect of PMA on removing Sn^{2+} was studied at different pH and P/M. The rejection of Sn^{2+} at different solution pH and P/M is shown in Fig. 4. It is observed that the Sn^{2+} removal rate increases with the increase of pH for all the P/M when the pH ranges from 2.0 to 5.5. This can be attributed to the stability of the formed PMA-Sn complex which is pH dependent. Rivas et al. [34,35] suggested that hydrogen ions would compete with metal ions to remain on the surface of polymer molecules. The competitive mechanism can be described by the following equilibrium reactions:

$$[\text{-COO}]^- + H^+ \rightleftharpoons [\text{-COOH}] \tag{5}$$

$$2[\text{-COO}]^- + Sn^{2+} \rightleftharpoons [\text{-COO}]_2Sn \tag{6}$$

According to Reaction (5) and (6), at low pH, the affinity of PMA towards the Sn^{2+} is weak due to the presence of most hydrogen ions and so most of Sn^{2+} still stay the form of free ions in the aqueous solution through the ultrafiltration membrane, resulting in the rejection rate is not high. As pH continues increasing, the deprotonation degree of carboxylic group rises and more ionized carboxylic groups are available to bind metal ions, causing the rising of rejection of Sn^{2+}. As shown in Fig. 5, when pH exceeds 5.0 and P/M is increased to 5, the Sn^{2+} removal rate reaches a plateau
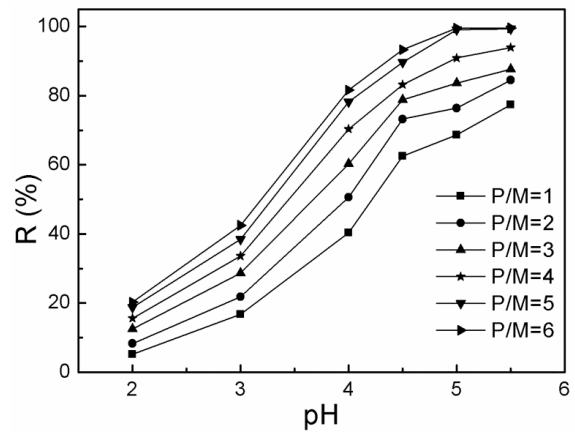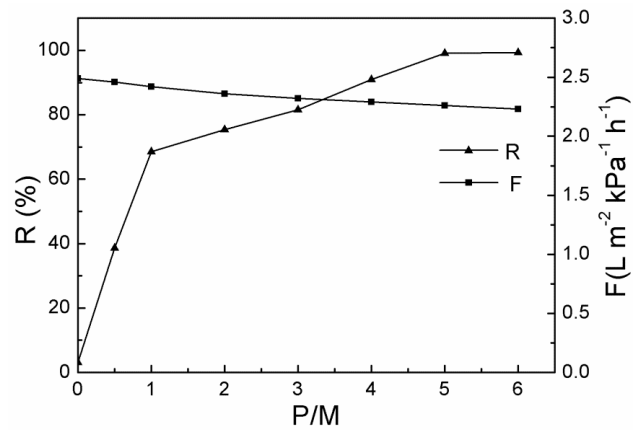

Fig. 5. Effect of P/M on the rejection of Sn^{2+} and the permeate flux of unit pressure (pH, 5.0; initial Sn^{2+} concentrations, 10 mg L^{-1}; rotating speed, 300 rpm; temperature, 25°C; initial pressure, 10 kPa).

and attains about 99%. The previous study [16,36] indicated that a sustained increase in pH will lead to the formation of hydroxides and cause decrease in permeate flux. Therefore, 5.0 is chosen as the optimum pH value.

The effect of P/M on rejection rate and permeate flux was examined at pH 5.0 under 300 rpm. The results are shown in Fig. 5. Evidently, the rejection of Sn^{2+} increases with the increasing of the P/M. The phenomenon may be explained as follows: with the improvement of the amount of PMA, the complex sites increases, leading to the result that the rejection of Sn^{2+} increased. When P/M was increased to 5, the Sn^{2+} in solution has been completely bound to PMA and the rejection of Sn^{2+} reached a plateau at 99.3%. Considering from both the tin removal rate and the economical cost of PMA, the optimum P/M is chosen to be 5.

The permeation coefficient F (L m^{-2} k Pa^{-1} h^{-1}) which is defined as permeate flux per unit transmembrane pressure. According to Darcy's law, the permeate flux per unit transmembrane pressure can be expressed as the following formulas:

$$F = \frac{J}{\Delta P} = \frac{1}{(\mu R_t)} \qquad (7)$$

$$R_t = R_m + R_f + R_c \qquad (8)$$

As shown in Fig. 5, the F has a slightly decrease as P/M increases from 0 to 6. Effect of P/M on the relative viscosity (μ/μ_0) and membrane resistance at 300 rpm is displayed in Fig. 6, where μ and μ_0 is the viscosity of the solution and pure water, respectively. With the increase of the P/M, the relative viscosity rose slightly and the ratio of total resistance to the membrane intrinsic resistance (R_t/R_m) is almost 1.0. The results demonstrate that the decrease of F was only caused by the increase of the solution viscosity. R_f and R_c can be neglected due to the strong shear action on the membrane surface caused by rotating disk membrane module, which agrees with previous study [37,38].

3.3. The stability of PMA and PMA-Sn complex in the shear field

As one of the most important factor in industrial applications of complexation-ultrafiltration, the shear stabilities of PMA and PMA-Sn complex were investigated. The variation of the rejection of PMA with rotating speed at various pHs is shown in Fig. 7. From Fig. 7, the rejection of PMA was basically unchanged at about 96% when the rotating disk speed rise from 0 rpm to 3000 rpm, and further indicate that the structure of PMA maintained stable in the shear field. Additionally, since there still remained very few PMA whose molecular weight is smaller than MWCO in pre-treated PMA, which is due to the PMA rejection is slightly lower than 100%. Therefore, the stability of the polymer does not affect the application of complexation-ultrafiltration in industry.

Fig. 8 shows the variation of rejection of Sn^{2+} with rotating speed ranging from 0 to 3000 rpm when the P/M 5 at various pH values. The rejection of Sn^{2+} remains stable at low rotating speed, once the speed exceeds a certain value, the rejection of Sn^{2+} drops sharply. This indicates that the PMA-Sn complex is quickly dissociated to free metal ion

and can pass through the ultrafiltration membrane when the rotating speed is great enough, which can lead to the decline of the rejection rate. The critical rotating speed (N_c) is defined as the maximal speed within which the PMA-Sn complex can keep stable. It is clearly seen from Fig. 8, the critical rotating speeds at which the rejection of Sn^{2+} begins to decrease were 1960, 1680, 1520 rpm at pH values 5.0, 4.0, 3.0, respectively. Clearly, the shear stability of PMA-Sn complex will significantly improve with the increase of pH, this phenomenon has been reported in many kinds of literatures [29,30]. The deprotonation degree of carboxyl groups in PMA molecules is slight at low pH, thereby lacking sufficient ligands that bind to metal ions. In higher pH value, the deprotonation degree of carboxyl groups will be greatly improved, which causes a large amount of ligands to be present in the PMA molecules and drive the complexation reaction of deprotonated carboxyl group with Sn^{2+}. Thus, the higher rotating speed is necessary to make PMA-Sn complex dissociate at higher pH. In Fig. 9, PMA-Sn begins to dissociate at the same rotating speed when P/M is 1, 3 and 5. The results illustrate that the shear stability of the PMA-Sn is irrelevant to P/M.
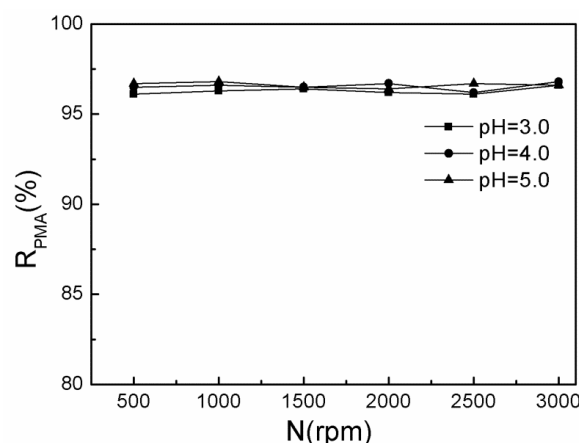

Fig. 7. Effect of rotating speed on the rejection of PMA at different pHs values (initial PMA, concentration, 200 mg L^{-1}; temperature, 25°C; initial pressure, 10 kPa).
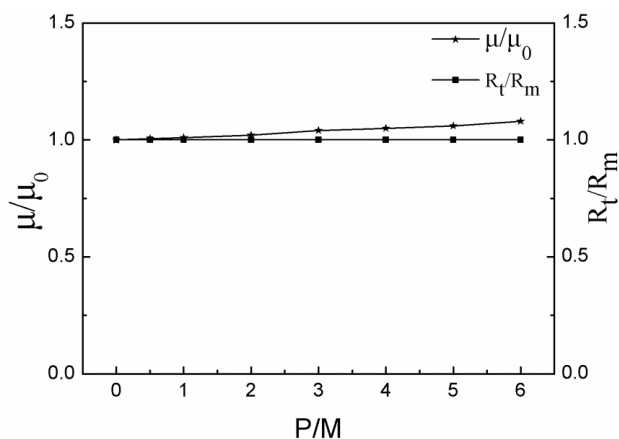

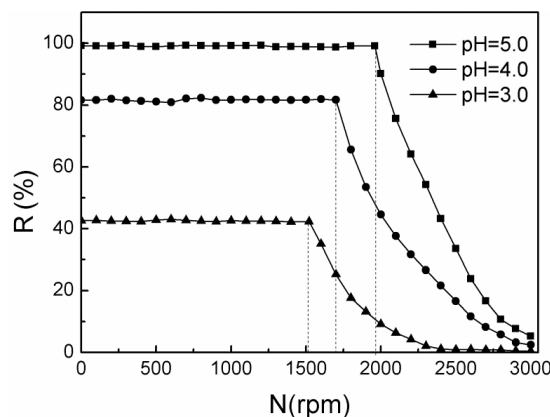Fig. 6. Effect of P/M on the relative viscosity and membrane resistance at 300 rpm.

Fig. 8. Effect of rotating speed on the rejection of Sn^{2+} at different pH values (P/M, 5; initial Sn^{2+} concentrations, 10 mg L^{-1}; temperature, 25°C; initial pressure, 10 kPa).

3.4. Determination of critical shear rate and critical shear radius

Generally, the shear field produced by different devices will not necessarily be the same even at the same rotating speed. In order to further explain the stability of the complex in the shear field, the critical shear rate (γ_c) of the PMA-Sn complex was studied. The critical shear rate is defined as the smallest shear rate at which the polymer-metal complex starts to dissociate. The shear rates (γ_m) on the membrane surface were calculated by Bouzerar et al. [39], which solved the axisymmetric Navier-Stokes equations using the similarity solution of Bodewadt in the laminar regime ($N \leq 570$ rpm) and turbulent regime ($N > 570$ rpm). The representations are as follow:

$$\gamma_{ml} = 0.77\upsilon^{-0.5}(k\omega)^{1.5} \tag{9a}$$

$$\gamma_{mt} = 0.0296\upsilon^{-0.8}(k\omega)^{1.8} r^{1.6} \tag{9b}$$

where γ_{ml} and γ_{mt} represent the shear rates generated by the rotating disk on the membrane at laminar and turbulent state, respectively. υ is kinematic viscosity of test fluid (m² s⁻¹). ω is the rotating speed of the disk. r is the radius of the membrane. k represents the velocity following factor whose value is equal to the ratio of the fluid velocity to the disk speed, and its value is only related to the geometry of the device. The k value of the rotating disk with six vanes using in this study is 0.796 according to the data taken from an earlier publication from our laboratory [24].

According to Eq. (9b), the critical shear rates of PMA-Sn complex were calculated as about 2.68×10^5, 2.15×10^5 and 1.67×10^5 s⁻¹ at the pH of 5.0, 4.0 and 3.0, respectively. Obviously, the critical shear rates of PMA-Sn increase along with pH, which indicated that the stability of PMA-Sn is pH dependent and increases with the increase of pH. This result is also consistent with the conclusion in the above section. In addition, the experimental results provide support for the following shear induced dissociation and ultrafiltration experiment.

The segmentation model on the membrane surface was established to reveal the distribution of PMA-Sn complex in the shear field. The distribution map of substances on the membrane surface is represented in Fig. 10. The critical shear radius (abbreviated as r_c) is defined as the boundary within which the polymer-metal complex can keep stable. When $r_c < r < r_m$, PMA-Sn is completely dissociated, and the concentration of the metal ions in the permeate is equal to the initial metal ions concentration (C_f). When $0 < r < r_c$, the PMA-Sn complex is stable and can be retained by the membrane, and the metal ions concentration in permeate is equal to the concentration of permeate in the static filtration at the same condition.

Tang et al. [27] obtained calculation formulas of critical shear radius by segmentation model and the principle of material balance, the representations are as follow:

$$r_c^4 + \frac{364P_0}{\rho k^2 N^2} r_c^2 + \frac{C_P - C_f}{C_f - C_0}\left(r_m^4 + \frac{364P_0}{\rho k^2 N^2} r_m^2\right) + \frac{C_0 - C_p}{C_f - C_0}\left(r_0^4 + \frac{364P_0}{\rho k^2 N^2} r_0^2\right) = 0 \tag{10}$$

where r_0 is the membrane inside radius, and it is 0.005 m. r_m is the outer radius of the membrane, and it is 0.088 m. C_p is the tin concentration in permeate when rotating disk enhancing complexation-ultrafiltration. C_0 is tin concentration in permeate at 0 rpm. ρ represents the density (kg·m⁻³)

of the solution. N is the rotating speed (rpm) and P_0 is the pressure at the symmetry axis.

The critical radius r_c can be obtained according to Eq. (10). Inserting the experimental data in Fig. 9 into Eq. (10), the relationship between the critical radius and the rotating speeds can be obtained in Fig. 11. The critical radius decreases with the increasing of rotating speed at a certain pH, indicating that the increase of rotating speed obviously
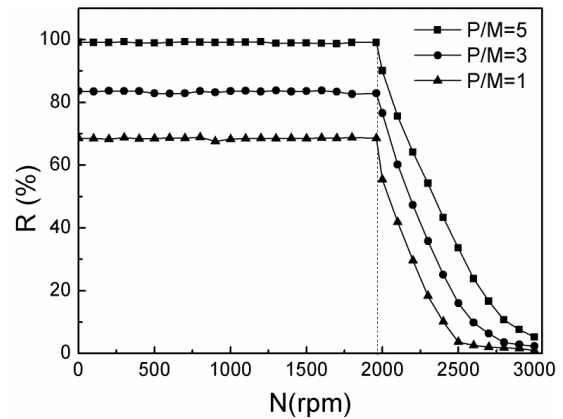
Fig. 9. Effect of rotating speed on the rejection of Sn²⁺ at different P/M values (pH, 5.0; initial Sn²⁺ concentrations, 10 mg L⁻¹; temperature, 25°C; initial pressure, 10 kPa).
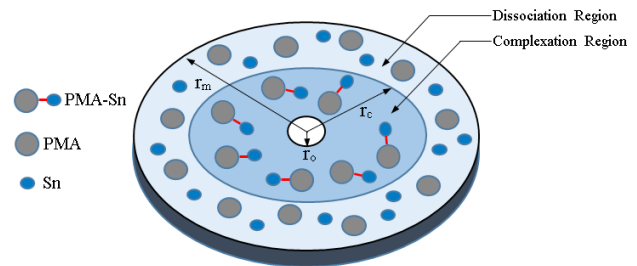
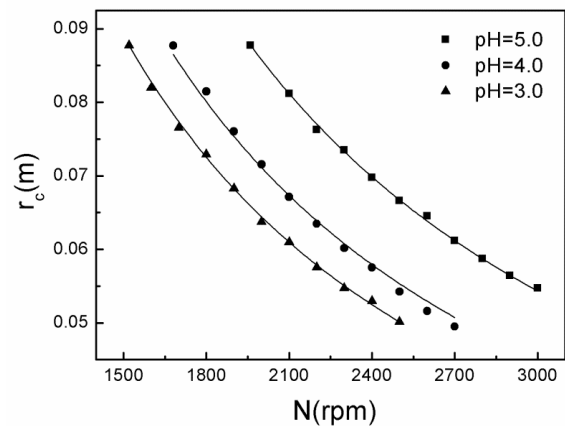Fig. 10. The distribution map of substances on the membrane surface (Inorganic anions and sodium omitted).

Fig. 11. The relationships between the critical radius and the rotating speed at different pHs.

Table1
γ_c of PMA-Sn complex and correlations of r_c and N at various pHs

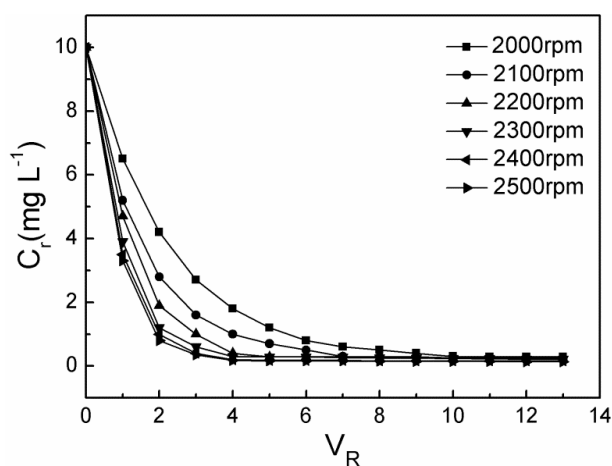| pH	Nc (rpm)	γ_c (s⁻¹)	Fitting equation	Regression coefficient (R²)
3.0	1520	1.67×10^5	$r_c = 333.1028 N^{-1.125}$	0.9991
4.0	1680	2.15×10^5	$r_c = 367.8924 N^{-1.125}$	0.9989
5.0	1960	2.68×10^5	$r_c = 443.6605 N^{-1.125}$	0.9993

Fig. 12. Variations of the concentration of Sn²⁺ in the retentate with the volume ratio of supplementary deionized water to raw material at different rotating speeds (pH, 5.0; P/M, 5; initial Sn²⁺ concentrations, 10 mg L⁻¹; temperature, 25°C; initial pressure, 10 kPa).
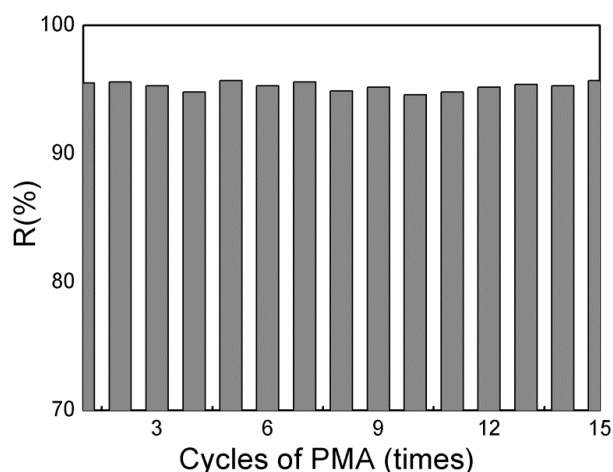

Fig. 13. Variations of the rejection of Sn²⁺ with different times of PMA cycles (pH 5.0; P/M5; initial Sn²⁺ concentrations, 10 mg L⁻¹; temperature, 25°C; initial pressure, 10 kPa).

extends the scope of the dissociation region. In addition, the fitted results of r_c and N at different pH are shown in Table 1.

The experimental data of Section 3.3 and Section 3.4 confirm that the reason why the efficiency of complex-ultrafiltration technology in industrial applications is low: the high shear rate generated by the blades of the centrifugal pump causes the dissociation of polymer-metal complex. According to the Section 3.1, it takes about 35 min for Sn²⁺ to get the complexation equilibrium. However, it takes much less than 5 min for the fluid to leave from the centrifugal pump to the membrane module in industrial wastewater treatment. Thus, only a minority of the dissociated polymer can react again with Sn²⁺, and result from remarkable reduction in rejection. Practically, the critical shear rate and radius obtained in this study will provide some guidance for the industrialization process of complexation-ultrafiltration technology, especially, the choice of centrifugal pump parameters in the process of conveying raw materials.

3.5. Recovery of PMA and Sn²⁺ using shear induced dissociation and ultrafiltration

According to the Section 3.3, PMA-Sn complex will dissociate exceeding a certain speed, so we can utilize this property of shear induced dissociation to recover Sn²⁺ and PMA. Based on the result of preliminary test, this experiment was carried out under the condition of P/M 5 and pH 5.0. For the purpose of separating PMA and tin, we controlled the speed to a certain speed at which the PMA-Sn complex could dissociate. Then, on the premise of the constant volume of the raw material, the permeate was continuously discharged, and deionized water was added to it as well. The Sn²⁺ dissociated from PMA-Sn complex can pass through the membrane to achieve the separation effect. The result is shown in Fig. 12. V_R represents the volume ratio of supplementary deionized water to raw material and C_r represents the concentration of Sn²⁺ in retentate. It can be evidently seen that the speed of dissociation increase with the improvement of the rotating speeds. When the tin content in the retentate is minimal, the V_R reached 4.0 and remained nearly constant at rotating speed exceeded 2200 rpm. Because the larger electric power is needed to provide higher rotating speed, comprehensive consideration, 2200 rpm ($\gamma = 3.28 \times 10^5$ s⁻¹) is determined as the best rotating speed for shear induced dissociation to recover Sn²⁺ and PMA.

Moreover, the regenerated PMA was used to remove Sn²⁺ at the optimal condition. PMA was regenerated for 15 times, and Fig. 13 shows the effect of PMA cycles on the rejection of Sn²⁺. It is clearly seen from Fig. 13, the rejection of Sn²⁺ are all attained more than 95% using regenerated PMA, which diminished not too much compared to 99.3% of original PMA. This confirms that the regenerated PMA still has excellent complexing performance. By measuring the concentration of PMA in the permeate and retentate, it is found that there is almost no PMA with low molecular in re-used PMA after the first SIDU experiments. Therefore, the total amount of

PMA will not decrease again after several cycles of PMA. However, the Sn^{2+} rejection of regenerated PMA is still comparatively lower than that of original PMA, it can be explain that the rotating speed for PMA regeneration is 2200 rpm, there still exists a small complexation region near the center according to Fig. 10, which lets very little PMA-Sn complex exist in regenerated PMA.

4. Conclusions

Commercially available polymer, the copolymer of maleic acid and acrylic acid, was used for the efficient removal of Sn^{2+} from aqueous solutions by complexation-ultrafiltration process using a rotating disk membrane. The optimum conditions of complexation between PMA and Sn^{2+} were pH = 5.0, P/M = 5, at which the rejection of Sn^{2+} reached 99.3%. The kinetics of complexation reactions of PMA with Sn^{2+} was investigated. It takes 35 min for Sn^{2+} to get the complexation equilibrium, and the reaction kinetics can be described by a pseudo-first-order equation. The stability of PMA and PMA-Sn in the shear field was studied, results show that PMA could keep stable within the rotating speed of 3000 rpm and pH has little effect on its stability in the shear field. However, PMA-Sn complex will start to dissociate at the rotating speed of 1520, 1680 and 1960 rpm at pH 3.0, 4.0 and 5.0, respectively. Then, by the segmentation model and the principle of material balance, the critical shear rates of PMA-Sn were calculated as about 1.67×10^5, 2.15×10^5 and 2.68×10^5 s^{-1} at pH 3.0, 4.0 and 5.0, respectively. Most importantly, the method of shear-induced dissociation and ultrafiltration was effectively applied to recover tin and regenerate PMA, and the performance of regenerated PMA is good. The experimental results indicate that shear induced dissociation is a promising technology for recovering tin and regenerating PMA.

Symbols

C_f	—	Initial Sn^{2+} concentration (mg L^{-1})
C_0	—	Sn^{2+} concentration in permeate at rest (mg L^{-1})
C_p	—	Sn^{2+} concentration in permeate (mg L^{-1})
C_r	—	Sn^{2+} concentration in retentate (mg L^{-1})
F	—	Permeation coefficient(L m^{-2} kPa^{-1} h^{-1}, m s^{-1} Pa^{-1})
J	—	Permeate flux (L m^{-2} h^{-1}, m s^{-1})
k	—	Rate constant (Eq. 1); velocity following factor (Eq. 9)
k^*	—	Observed rate constant
N	—	Rotating speed (rpm)
P_0	—	Center pressure (Pa)
r_m	—	Membrane outsider radius (m)
r_0	—	Membrane insider radius (m)
r_c	—	Critical radius (m)
R	—	Rejection of Sn^{2+} (%)
R^2	—	Regression coefficient
R_t	—	Total resistance (m^{-1})
R_m	—	Membrane resistance (m^{-1})
R_f	—	Membrane fouling (m^{-1})
R_c	—	Concentration polarization resistance (m^{-1})
t	—	Time (s)
V_R	—	The volume ratio of supplementary deionized water to raw material

Greek

μ	—	The viscosity of the solution (Pa s)
ν	—	Kinematic viscosity (m^2 s^{-1})
μ_0	—	The viscosity of pure water (Pa s)
ρ	—	Fluid density (kg m^{-3})
γ_c	—	Critical shear rate (s^{-1})
γ_m	—	Shear rate on membrane surface (s^{-1})
γ_{ml}, γ_{mt}	—	Shear rate on membrane surface in the laminar regime and turbulent regime (s^{-1})
ω	—	Angular velocity (rad s^{-1})

References

[1] M. Hoch, Organotin compounds in the environment-an overview, Appl. Geochem., 16 (2001) 719–743.

[2] FENT, Organotin compounds in municipal wastewater and sewage sludge: contamination, fate in treatment process and ecotoxicological consequences, Sci. Total Environ., 185 (1996) 151–159.

[3] P.L. Podratz, E. Merlo, G.C. Sena, M. Morozesk, M.M. Bonomo, S.T. Matsumoto, M.B. Da Costa, G.C. Zamprogno, P.A.A. Brandão, M.T.W.D. Carneiro, Accumulation of organotins in seafood leads to reproductive tract abnormalities in female rats, Reprod. Toxicol., 57 (2015) 29–42.

[4] A. Pagliarani, S. Nesci, V. Ventrella, Toxicity of organotin compounds: shared and unshared biochemical targets and mechanisms in animal cells, Toxicol. Vitr. An Int. J. Publ. Assoc. with Bibra., 27 (2013) 978–990.

[5] G.Z. Kyzas, P.I. Siafaka, E.G. Pavlidou, K.J. Chrissafis, D.N. Bikiaris, Synthesis and adsorption application of succinyl-grafted chitosan for the simultaneous removal of zinc and cationic dye from binary hazardous mixtures, Chem. Eng. J., 259 (2015) 438–448.

[6] T.J. Afolabi, A.O. Alade, M.O. Jimoh, I.O. Fashola, Heavy metal ions adsorption from dairy industrial wastewater using activated carbon from milk bush kernel shell, Desal. Water Treat., 57(31) (2016) 14565–14577.

[7] A. Imyim, C. Thanacharuphamorn, A. Saithongdee, F. Unob, V. Ruangpornvisuti, Simultaneous removal of Ag(I), Cd(II), Cr(III), Ni(II), Pb(II), and Zn(II) from wastewater using humic acid-coated aminopropyl silica gel, Desal. Water Treat., 57(37) (2016) 17411–17420.

[8] A. Mittal, R. Ahmad, I. Hasan, Iron oxide-impregnated dextrin nanocomposite: synthesis and its application for the biosorption of Cr(VI) ions from aqueous solution, Desal. Water Treat., 57(32) (2016) 15133–15145.

[9] M.G. Kiran, K. Pakshirajan, G. Das, A new application of anaerobic rotating biological contactor reactor for heavy metal removal under sulfate reducing condition, Chem. Eng. J., 321 (2017) 67–75.

[10] H.Y. Yen, P.L. Chen, Adsorption of Cd(II) from wastewater using spent coffee grounds by Taguchi optimization, Desal. Water Treat., 57(24) (2016) 11154–11161.

[11] M.K. Uddin, A review on the adsorption of heavy metals by clay minerals, with special focus on the past decade, Chem. Eng. J., 308 (2017) 438–462.

[12] L. Dambies, A. Jaworska, G. Zakrzewskatrznadel, B. Sartowska, Comparison of acidic polymers for the removal of cobalt from water solutions by polymer assisted ultrafiltration, J. Hazard. Mater., 178 (2010) 988–993.

[13] J.X. Zeng, H.Q. Ye, Z.Y. Hu, Application of the hybrid complexation-ultrafiltration process for metal ion removal from aqueous solutions, J. Hazard. Mater., 161 (2009) 1491–1498.

[14] Y. Huang, J.R. Du, Y. Zhang, D. Lawless, X. Feng, Removal of mercury (II) from wastewater by polyvinylamine-enhanced ultrafiltration, Sep. Purif. Technol., 154 (2015) 1–10.

[15] Y. Huang, D. Wu, X. Wang, W. Huang, D. Lawless, X. Feng, Removal of heavy metals from water using polyvinylamine by polymer-enhanced ultrafiltration and flocculation, Sep. Purif. Technol., 158 (2016) 124–136.

[16] G. Borbély, E. Nagy, Removal of zinc and nickel ions by complexation-membrane filtration process from industrial wastewater, Desalination, 240 (2009) 218–226.

[17] H. Ouni, The effect of surfactant on dye removal by polyelectrolyte enhanced ultrafiltration, Desal. Water Treat., 56(6) (2015) 1526–1535.

[18] D.J. Ennigrou, M.B.S. Ali, M. Dhahbi, M. Ferid, Removal of heavy metals from aqueous solution by polyacrylic acid enhanced ultrafiltration, Desal. Water Treat., 56(10) (2015) 2682–2688.

[19] C.W. Li, C.H. Cheng, K.H. Choo, W.S. Yen, Polyelectrolyte enhanced ultrafiltration (PEUF) for the removal of Cd(II): Effects of organic ligands and solution pH, Chemosphere, 72 (2008) 630–635.

[20] Y. Zhang, Z. Xu, Study on the treatment of industrial wastewater containing Pb^{2+} ion using a coupling process of polymer complexation-ultrafiltration, Sep. Purif. Technol., 38 (2003) 1585–1596.

[21] J.J. Porter, Recovery of polyvinyl alcohol and hot water from the textile wastewater using thermally stable membranes, J. Membr. Sci., 151 (1998) 45–53.

[22] H. Zhao, S. Zhang, Removal of 2,4,6-trinitrotoluene from wastewater using a novel adsorbent polyvinyl alcohol/SiO_2, Desal. Water Treat., 52 (2014) 5983–5989.

[23] Y.R. Qiu, L.J. Mao, W.H. Wang, Removal of manganese from waste water by complexation–ultrafiltration using copolymer of maleic acid and acrylic acid, Trans. Nonferrous Met. Soc., 24 (2014) 1196–1201.

[24] Y.R. Qiu, L.J. Mao, Removal of heavy metal ions from aqueous solution by ultrafiltration assisted with copolymer of maleic acid and acrylic acid, Desalination, 329 (2013) 78–85.

[25] J.W. Nicholson, Metal salts interaction with acrylic acid–maleic acid copolymer: An infrared spectroscopic study, J. Appl. Polym. Sci., 78 (2015) 1680–1684.

[26] L.P. Buckley, S. Vijayan, G.J. McConeghy, S.R. Maves, J.F. Martin, Removal of soluble toxic metals from water, At. Energy Canada Limited, AECL, 90 (1990) 1544–1590.

[27] S.Y. Tang, Y.R. Qiu, Removal of copper(II) ions from aqueous solutions by complexation–ultrafiltration using rotating disk membrane and the shear stability of PAA-Cu complex, Chem. Eng. Res. Des., 136 (2018) 712–720.

[28] S. Tang, Y. Qiu, Removal of Zn (II) by complexation-ultrafiltration using rotating disk membrane and the shear stability of PAA-Zn complex, Korean J. Chem. Eng., 35 (2018) 2078–2085.

[29] J. Gao, Y. Qiu, B. Hou, Q. Zhang, X. Zhang, Treatment of wastewater containing nickel by complexation-ultrafiltration using sodium polyacrylate and the stability of PAA-Ni complex in the shear field, Chem. Eng. J., 334 (2018) 1878–1885.

[30] Z.J. Xian, Y.H. Qi, H. Nian Dong, L. Jun Feng, Z.L. Feng, Selective separation of Hg(II) and Cd(II) from aqueous solutions by complexation-ultrafiltration process, Chemosphere, 76 (2009) 706–710.

[31] R. Molinari, P. Argurio, T. Poerio, G. Gullone, Selective separation of copper(II) and nickel(II) from aqueous systems by polymer assisted ultrafiltration, Desalination, 200 (2006) 728–730.

[32] R. Molinari, P. Argurio, Arsenic removal from water by coupling photocatalysis and complexation-ultrafiltration processes: A preliminary study, Water Res., 109 (2017) 327–336.

[33] H. Ishii, M. Yamaguchi, T. Odashima, Studies on complexation equilibria between water-soluble hydrazones which consist of 5-nitro-2-pyridylhydrazine and heterocyclic ketones and divalent metal ions, Talanta., 39 (1992) 1181–1188.

[34] P. Cañizares, A. Pérez, R. Camarillo, R. Mazarro, Simultaneous recovery of cadmium and lead from aqueous effluents by a semi-continuous laboratory-scale polymer enhanced ultrafiltration process, J. Membr. Sci., 320 (2008) 520–527.

[35] X.L. Shi, F.M. Xu, Z.J. Zhang, Y.L. Dong, Y. Tan, L. Wang, J.M. Yang, Mechanical properties of hot-pressed Al_2O_3/SiC composites, Mat. Sci. Eng., 527 (2010) 4646–4649.

[36] J. Huang, F. Yuan, G. Zeng, X. Li, Y. Gu, L. Shi, W. Liu, Y. Shi, Influence of pH on heavy metal speciation and removal from wastewater using micellar-enhanced ultrafiltration, Chemosphere, 173 (2017) 199–206.

[37] J. Luo, Z. Zhu, L. Ding, O. Bals, Y. Wan, M.Y. Jaffrin, E. Vorobiev, Flux behavior in clarification of chicory juice by high-shear membrane filtration: Evidence for threshold flux, J. Membr. Sci., 435 (2013) 120–129.

[38] W. Zhang, L. Ding, N. Grimi, M.Y. Jaffrin, T. Bing, Application of UF-RDM (Ultafiltration Rotating Disk Membrane) module for separation and concentration of leaf protein from alfalfa juice: Optimization of operation conditions, Sep. Purif. Technol., 175 (2017) 365–375.

[39] R. Bouzerar, L. Ding, M.Y. Jaffrin, Local permeate flux-shear-pressure relationships in a rotating disk microfiltration module: implications for global performance, J. Membr. Sci., 170 (2000) 127–141.